

# **Ground Based Remote Sensing of Snow Properties and Avalanche Simulation**

**Rudolf Sailer, Reinhard Fromm, Philipp Jörg, Andreas Schaffhauser, Marc Adams**

Federal Research and Training Centre for Forests, Landscape and Natural Hazards, Austria

## **Abstract**

At present avalanche simulation models are commonly used for hazard mapping and in risk and crisis management. For the improvement and verification of simulation models a detailed information of the avalanche formation, extension and flow behaviour is essential. Therefore full scale avalanche experiments are undertaken. The GALAHAD (Advanced Remote Monitoring Techniques for Glaciers, Avalanches and Landslides Hazard Mitigation) study area is situated in "Wattener Lizum", Tuxer Alpen, Tyrol, Austria. GALAHAD is a Specific Targeted Research Project under the European Commission FP6-2004-Global-3 (Project No. 018409). TLS (Terrestrial Laser Scanning) measurements as well as GB-SAR (Ground-based Synthetic Aperture Radar) interferometry are used to derive snow cover properties in a high temporal and spatial resolution. Avalanches are artificially released and observed with remote monitoring instruments.

TLS measurements (which have been verified by in situ field observations) prior to and after the events give avalanche mass balance information. It is observed that the deposited snow mass ( $58.3 \times 10^6$  kg) of an avalanche artificially triggered on 25<sup>th</sup> April 2008 exceeds the release mass ( $-19.6 \times 10^6$  kg) significantly. The difference of  $-38.7 \times 10^6$  kg is attributed to the incorporation of snow during the event (entrainment). This information (e.g. release mass of the avalanche, potential entrainment mass) is used as an input for the avalanche simulation model SamosAT (Snow Avalanche MOdelling and Simulation). Subsequently, model improvements and adjustments of the default parameter set are achieved. Based on the measured avalanche parameters (release mass, entrainment mass, deposition mass) an adequate optimization of simulation parameters were achieved. It is shown that the runout of an artificially triggered avalanche can only be recalculated by introducing two additional model parameters (the minimum shear stress and the entrainment resistance force).

**Key words: avalanche simulation, avalanche mass balance, terrestrial laser scanning**

# 1. Introduction

In winter sport destinations the responsible persons for safety (politicians, members of avalanche commissions or warning centres) are faced with the challenge of assessing the risk of natural hazards. In Austria the authority to act is assigned to the municipality (mayor, council) by law (Khakzadeh 2004). Within the last decades, due to the tourist rush into Alpine rural regions, the population density increased significantly during high season. In Tyrol (Western Austria) the maximum population can reach urban values of >600 individuals per square kilometre (TIRIS 2007). The reaction of the public authorities to this challenge is manifold. In addition to the extraordinary expenditures for direct protection and defence structures (in Austria: between 1949 and 1989 350 Million Euros; between 1999 and 2003 120 Million Euros) temporary measures (road blocks, evacuations, avalanche blasting, work of avalanche warning centres and avalanche commissions) gain in importance. In summary, a comprehensive risk and crisis management at a regional or local level – also in rural areas – has to take into account i) the increasing number of exposed people during high season and ii) the new aspects brought forth by temporary measures.

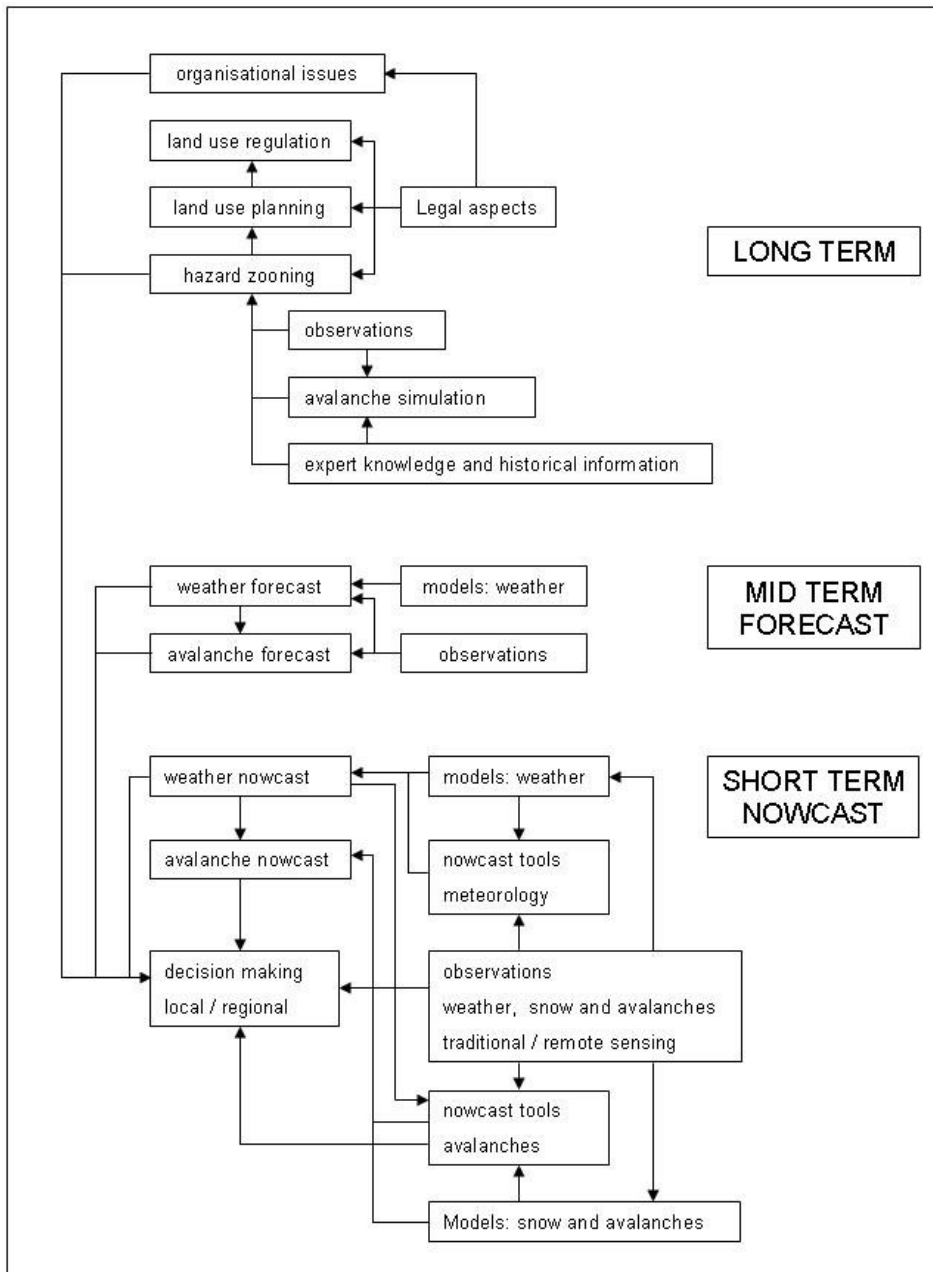


Figure 1. Components of Long Term Forecast, Mid Term Forecast and Short Term nowcast in risk and crisis management with particular regard to avalanches.

The prognosis time span (long term, mid term, short term) in risk and crisis management, determines the choice and combination of measures (Figure 1.). Elements of a long term forecast (e.g. land use planning) are generally based on laws, which manifest the need to consider natural hazards. In Austria hazard zoning is regulated by forest law and has to take place wherever natural hazards are of significance. In avalanche risk and crisis management the midterm forecast is conducted mainly with weather forecast. World wide efforts were undertaken to improve the midterm (several days) forecast of snow fall and its regional distribution. nowcasting weather as well as avalanches has to be done within a few hours or even during critical situations to support stakeholders with crucial weather and avalanche information. Not only in hazard zoning but also in the field of nowcasting, avalanche simulation models gain in importance (Huber and Sailer 2005). Beside the well established one dimensional avalanche simulation model AVALID (Salm et al. 1990) two and three dimensional models are in operational use. In Austria, for example, SamosAT (Sampl and Zwinger 2004, Zwinger et al. 2003, Sailer et al. 2002, Sailer et al. 2008) and ELBA+ (Volk 2004, Volk and Kleemayr 1999) are used supplementary to delineate avalanche hazard zones. In a risk and crisis management context avalanche simulation models are used to prepare various scenarios. Based on forecasted or measured snow fall amounts, combined with extreme value analysis, specific scenarios have to be chosen by the experts on a regional or local level (e.g. avalanche commission) (Sailer 2001a, 2001b, Sailer et al. 2004).

Due to their practical relevance and importance avalanche simulation models are subjected to a continuous improvement and scientific verification. In terms of scientific verification and optimization processes of avalanche simulation models, reliable input parameters (snow depth, snow density) are essential. Particularly terrestrial laser scanning (TLS) and ground based interferometric synthetic aperture radar (GB SAR) provide the capacities to measure snow depth as well as snow density in an adequate spatial and temporal resolution (Jörg et al. 2006, Luzi et al. 2007).

The focus of this paper lies on the utilisation of TLS measurements, which will be used to calculate the mass balance of an artificially released avalanche (April 25<sup>th</sup> 2007) and subsequently – based on this information – to optimize model parameters of the avalanche simulation model SamosAT. The measurements were carried out in the frame of the EU-funded GALAHAD (Advanced Remote Monitoring Techniques for Glaciers, Avalanches and Landslides Hazard Mitigation) project. For the snow and avalanche related section of GALAHAD a test site was instrumented in Wattener Lizum (Tyrol, Austria, Figure 2.).

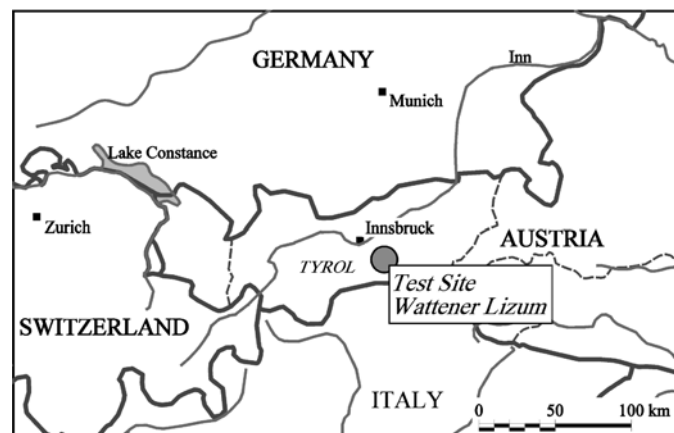


Figure 2. Location of Wattener Lizum test site (Tyrol, Austria).

This paper is divided into two main chapters. In chapter “2. Terrestrial Laser Scanning” the peculiarities of the artificially released avalanche are outlined, followed by the according TLS results (snow depth and snow depth changes), including the avalanche mass balance. The consecutive chapter “3. Avalanche Simulation with SamosAT” comprises the avalanche simulations, which have been primarily based on the input information gained from TLS. Results which have been based on two different optimization methods will be shown, followed by conclusions and an outlook in chapter 4.

## 2. Terrestrial Laser Scanning, Avalanche 25<sup>th</sup> April 2007

The test avalanche was artificially triggered by hand charge beneath “Tarntaler Köpfe” on April 25<sup>th</sup> 2007 at noon (Figure 3.). The avalanche successfully released at an altitude of approximately 2570 m a.s.l. on a North-East exposed slope. The runout length from the fracture line to the furthest deposition was about 1100 m, with a vertical fall height of 520 m. The release area is divided into two sub-release areas, as shown in Figures 3. and 4.

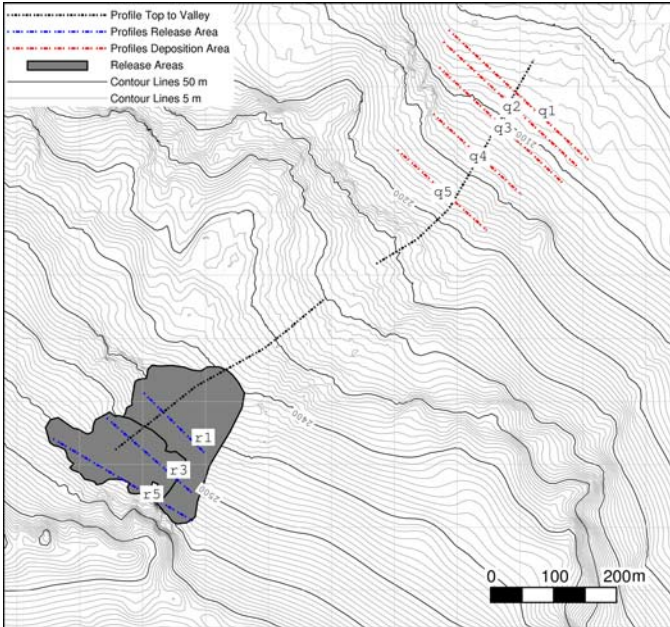


Figure 3. Wattener Lizum test site – avalanche area, release area, profiles in release area (r1, r3, r5) and deposition area (q1 to q5).

Figure 4. Avalanche release area right after the blasting (column of smoke). Two distinct release areas are visible – the upper one is already in motion, the lower one is just released (Photo: R. Fromm, BFW).

The projected size of the entire release area is 42000 m<sup>2</sup> (Upper Section 17000 m<sup>2</sup>, Lower Section 25000 m<sup>2</sup>). With a slope angle of about 35° the inclined area amounts to 51000 m<sup>2</sup>. Prior to and after the avalanche event, TLS measurements were carried out. The difference between both scans indicate a mean release depth of -0.97 m in the Upper Section and -0.92 m in the Lower Section. Figure 5. shows three cross profiles over the release area and refers to the TLS snow depth prior to and after the avalanche event and the difference between both TLS measurements. Before the avalanche was released the total – relatively homogeneously distributed – snow depth was approximately 2.0 m. It is evident that snow was predominantly eroded between the release fracture line at 2570 m a.s.l. and 2350 m a.s.l.. Only few accumulations are recorded (Figure 5. and 7.).

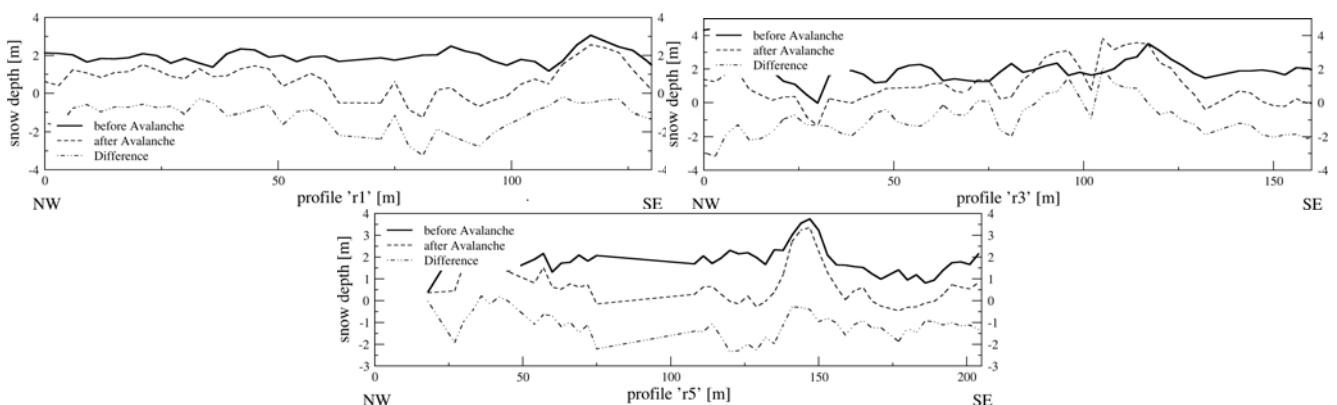


Figure 5. TLS snow depth prior to and after the avalanche event and the calculated difference over three cross profiles in the release area. The position of the cross profiles is shown in Figure 3.

Prior to the avalanche the measured snow depth in the runout zone was about 1.0 m and also homogeneously distributed (Figure 6.). The avalanche of April 25<sup>th</sup> caused an inhomogeneous redistribution of the snow mass over the runout zone, with snow depth maxima of approximately 5 m. Two main avalanche branches are depicted in Figures 6. (profiles q1 and q3) and Figure 7. The accumulation is concentrated in the lower part of the runout zone (altitude < 2150 m; profiles q1, q2 and q3). The accumulated snow decreases continuously at altitudes above 2150 m. At the South-Eastern edge of profiles q4 and particularly q5 (Figure 6.) negative differences appear. These negative values refer to massive snow erosion along a distinct gully on the South-Eastern fringe of the deposition zone (also visible in Figure 7. as a small elongated assembly of blue pixels).

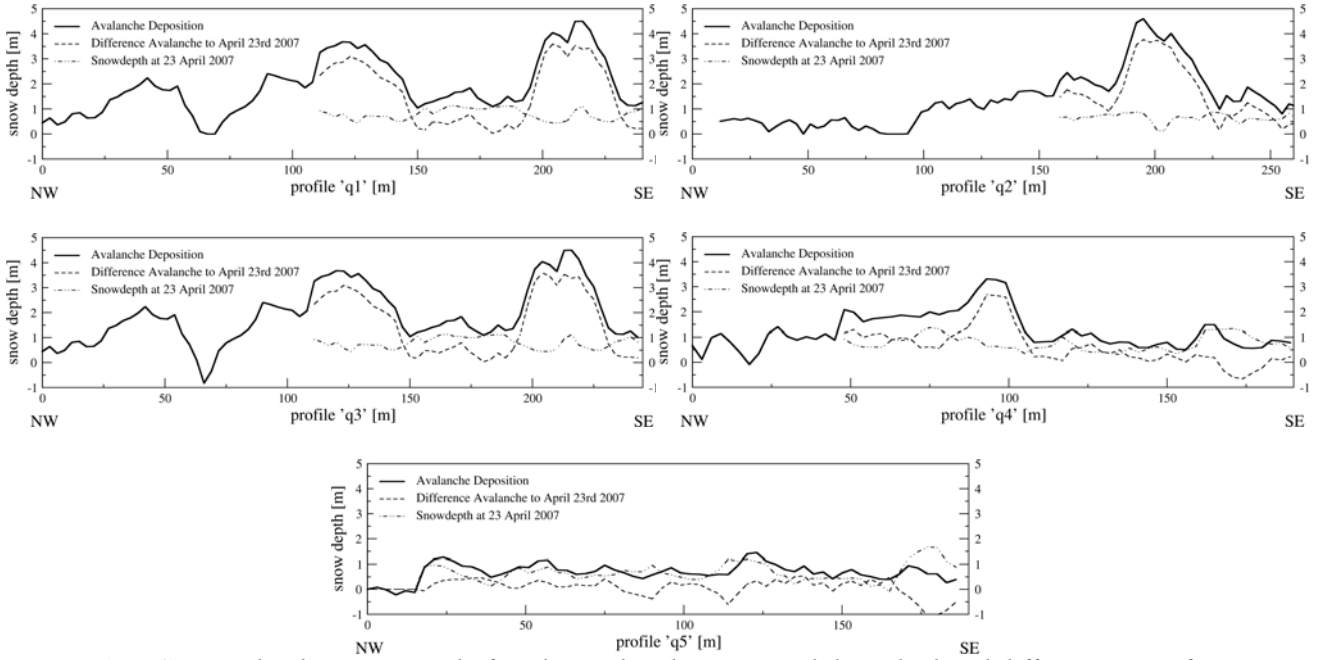


Figure 6. TLS snow depth prior to and after the avalanche event and the calculated difference over five cross profiles in the deposition area. The measured snow depth (23<sup>rd</sup> April 2007) did not cover the entire deposition zone. Therefore the snow depth and the difference values are partially missing in the North-Western part. The position of the cross profiles is shown in Figure 3.

For the calculation of the release mass, manual snow density measurements were carried out close to the release area and along the avalanche track one day after the event. Eight density core profiles lead to a mean snow density of  $450 \text{ kg m}^{-3}$  (minimum  $398 \text{ kg m}^{-3}$ , maximum  $470 \text{ kg m}^{-3}$ ) in the release area. The entire release mass  $M_R$  [kg]

$$M_R = p \overline{\rho^R} \sum_{i=1}^n \frac{d_i^R}{\cos\psi_i} \quad (1)$$

with the pixel size  $p$  [m] of  $n$  pixels of the release area, the mean release density  $\rho^R$  [ $\text{kg m}^{-3}$ ], the release depth  $d_i^R$  [m] and the slope angel  $\psi_i$  [ $^\circ$ ] amounts to  $-19.6 \times 10^6 \text{ kg}$ . Density core profiles were also taken from the deposition of the avalanche. As expected the mean density of the deposited snow  $\rho^D$  shows higher values and is approximately  $600 \text{ kg m}^{-3}$ . The deposition mass  $M_D$  [kg] for the observed avalanche is calculated with

$$M_D = p \overline{\rho^D} \sum_{i=1}^n \frac{d_i^D}{\cos\psi_i} \quad (2)$$

and triples with  $58.3 \times 10^6 \text{ kg}$  the value of  $M_R$  ( $d_i^R$  [m] is the deposition depth). If we define the mass balance  $B_M$  of an avalanche according to Sailer et al. (2008) with

$$B_M := M_D + M_R + M_E = p \overline{\rho^D} \sum_{i=1}^n \frac{d_i^D}{\cos\psi_i} + p \overline{\rho^R} \sum_{i=1}^n \frac{d_i^R}{\cos\psi_i} + M_E = 0 \quad (3)$$

and the entrainment mass  $M_E$  [kg] with

$$M_E := -(M_D + M_R) = -\left( p \overline{\rho^D} \sum_{i=1}^n \frac{d_i^D}{\cos\psi_i} + p \overline{\rho^R} \sum_{i=1}^n \frac{d_i^R}{\cos\psi_i} \right) \quad (3)$$

-38.7 x 10<sup>6</sup> kg snow was incorporated (entrained) into the avalanche mass along the track.

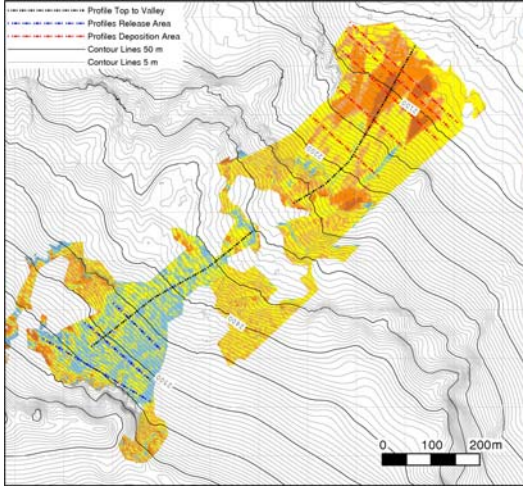


Figure 7. Snow depth changes from TLS measurements which were carried out prior and after the avalanche event.

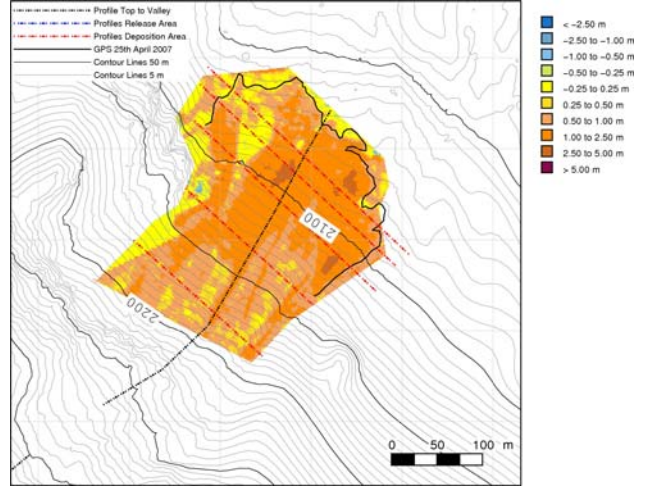


Figure 8. TLS snow depth after the avalanche event (difference to summer terrain).

### 3. Avalanche Simulation with SamosAT

The calculated release and entrainment mass were used to optimize two parameters i) the entrainment resistance force ( $F_{ent}$  [N m<sup>-2</sup>]) and ii) the minimal shear stress ( $\tau_0$  [N m<sup>-2</sup>]) of the avalanche simulation model SamosAT. The resistance force

$$F_{ent} = w_f (e^s + \overline{\rho_E} d_E e^d) \quad (4)$$

is needed to release snow from the ground and to compress it.  $e^s$  [J m<sup>-2</sup>] denotes the required breaking energy per fracture surface at the front width ( $w_f$  [m]). For simplification, deformation energy  $e^d$  (with entrainment density  $\rho_E$  [kg m<sup>-3</sup>] and entrainment depth  $d_E$  [m]) was set to zero during the optimization process. The two dimensional dense flow part of SamosAT (Zwinger et al. 2003, Sampl and Zwinger 2004) uses a modified model for the bottom friction, where the bottom shear stress  $\tau_b$  [N m<sup>-2</sup>], directed against the flow direction, is defined as

$$\tau_b = \tau_0 + \mu p_b + c_{dyn} \rho u^2, \quad (5)$$

with  $\mu$  the coefficient of Coulombian friction,  $p_b$  the normal pressure at the bottom,  $\rho$  the bulk density (here fixed to a constant value of 200 kg m<sup>-3</sup>),  $u$  the bulk velocity and  $c_{dyn}$  a turbulent friction coefficient. For further details concerning SamosAT and the parameter optimization we refer to Sailer et al. (2008).

Two acceptable parameter combinations have emerged throughout the parameter optimization. Combination N shows with  $e^s = 1652$  J m<sup>-2</sup> and  $\tau_0 = 1125$  N m<sup>-2</sup> slightly smaller values for the parameters than combination GN ( $e^s = 1998$  J m<sup>-2</sup> and  $\tau_0 = 1177$  N m<sup>-2</sup>). Considering only the runout length both combinations lead to satisfying results (Figures 9. and 10.). An improved distribution of the deposition mass is achieved with parameter combination GN, with maximum deposition values upside the maximal outline (Figure 11.), reflecting the real distribution slightly better. The calculated lateral spreading of both

combinations is in good agreement with the actual width of the avalanche. Furthermore, an intermediate deposition zone at the right boundary between 2200 m and 2230 m is reproduced by SamosAT (Figures 7., 9. and 10.).

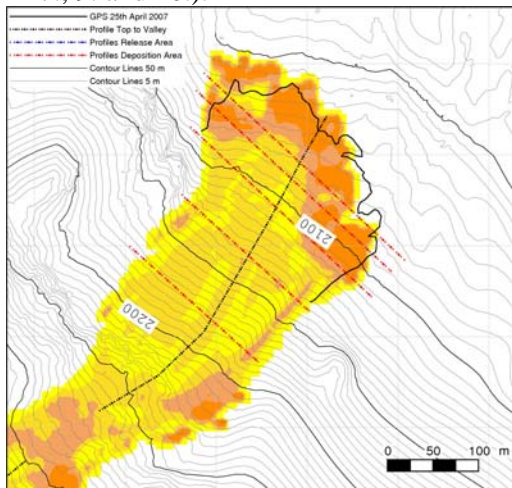


Figure 9. Snow depth calculated with SamosAT parameter combination N ( $e^s=1652 \text{ J m}^{-2}$  and  $\tau_0=1125 \text{ N m}^{-2}$ ).

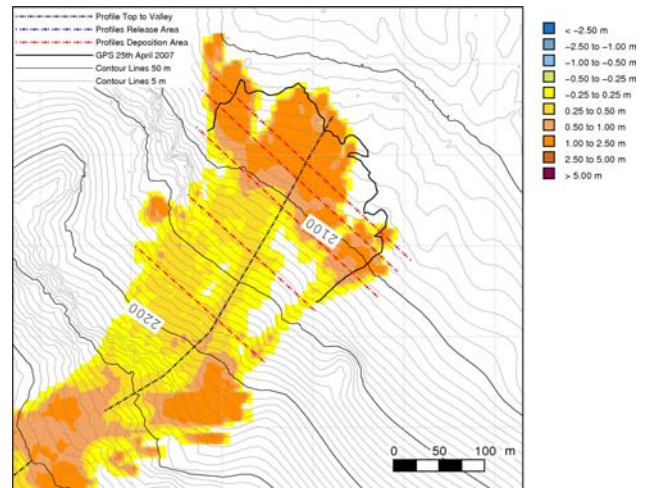


Figure 10. Snow depth calculated with SamosAT parameter combination GN ( $e^s=1998 \text{ J m}^{-2}$  and  $\tau_0=1177 \text{ N m}^{-2}$ ).

#### 4. Conclusions and Outlook

Detailed studies, carried out in the frame of the GALAHAD project in Wattener Lizum, lead to the assumption that TLS measurement deliver acceptable values to calculate the mass balance of avalanches. The analysed data sets are consistent and provide a satisfying image of the observed situations, before and after the avalanche on April 25<sup>th</sup> 2007. The data verification process and the results are described in Schaffhauser et al. (submitted) in detail.

Hence, the TLS data are usable for the parameter optimization of avalanche simulation models like SamosAT. Although the runout distance is well reflected by using the above mentioned parameter combinations, an unrealistic concentration of the avalanche mass is evident. In nature the avalanche mass was uniformly distributed along the runout zone (Figure 11.). The authors attribute the observed divergence to the basic depth-averaged (shallow water) model assumptions of the simulation model SamosAT. Furthermore the described parameter optimization (Chapter 3), is a first step to overcome the observed deviations of bulk mass accumulations (Sailer et al. 2008). Such optimized parameter sets of simulation models allow more reliable avalanche calculations and make a fundamental contribution to risk and crisis management operations at all fore- and nowcasting stages.

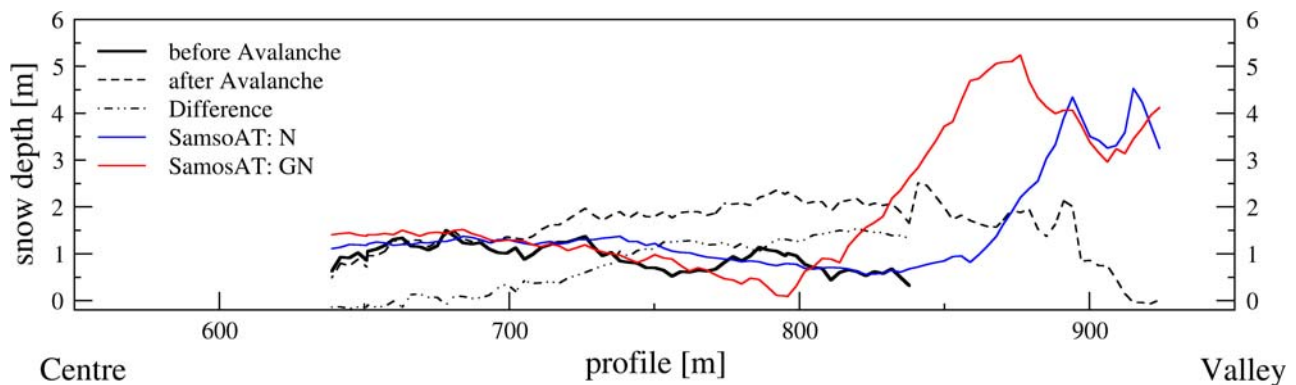


Figure 11. TLS snow depth and snow depth differences along the centre to valley profile (position is shown in Figure 3.). At this section the snow depth calculated with SamosAT combinations N and GN are plotted against the real (TLS) snow depth.

## Acknowledgements

The GALAHAD project is funded by the European Union (Specific Targeted Research Project FP6-2004-Global-3, Project N. 018409). The authors would like to thank colonel Knoll, commander of the military training camp in Wattener Lizum, and his team for the kind support. We appreciate the correction work done by Antonia Zeidler.

## References

- Huber T. and R. Sailer (2005). Regionalstudie Lebensraum "Hinteres Pitztal" . Wildbach- und Lawinenverbau. 2005, 153, 75-113.
- Jörg P., Fromm R., Sailer R., and A. Schaffhauser (2006) Measuring snow depth with a Terrestrial Laser Ranging System. ISSW 2006, Telluride, Colorado, USA. 452-460.
- Khakzadeh L. (2004) Rechtsfragen des Lawinenschutzes. NWV, Wien Graz. 174 pp.
- Luzi, G., Pieraccini, M., Noferini, L., Mecatti, D., Macaluso, G., Atzeni, C., Jörg, P. and R. Sailer. 2007. Microwave Interferometric Measurements Over a Snow Covered Slope: An Experimental data Collection in Tyrol (Austria), Proceedings of IGARSS 2007 Barcelona, Spain.
- Sailer, R., Rammer, L., and P. Sampl (2002). Recalculation of an artificially released avalanche with SAMOS and validation with measurements from a pulsed Doppler radar. NHESS, 2, 211-216.
- Sailer, R. (2001a) Risk Assessment and Crisis Management for a winter tourist resort (St.Anton a/A, Tyrol, Austria) - a case study (Part I). Proceedings of 21st ESRI Int. User Conference. San Diego, USA. 2001.
- Sailer, R. (2001b) Risk Assessment and Crisis Management for a winter tourist resort (St.Anton a/A, Tyrol, Austria) - a case study (Part II). Proceedings of the First Annual IIASA-DPRI Meeting on Integrated Disaster Risk Management: Reducing Socio-Economic Vulnerability. IIASA, Laxenburg, Austria. 2001.
- Sailer, R., Klebinder, K., Khakzadeh, L., and A. Heller (2004) Integraler Risiko- und Krisenmanagementplan der Gemeinde St. Anton am Arlberg. in: Strobl, J., Blaschke, T., and Griesebner, G. Beiträge zum 16. AGIT-Symposium Salzburg , Salzburg, 579-584.
- Sailer, R., Fellin, W., Fromm, R., Jörg, P., Rammer, L., Sampl, P., and A. Schaffhauser (2008). Snow avalanche mass balance calculation and simulation model verification. Annals of Glaciology, 48, in press.
- Salm B., Burkhard A. und H. U. Gubler (1990) Berechnung von Fließlawinen. Eine Anleitung für Praktiker mit Beispielen. Mitteilungen des Eidgenössischen Instituts für Schnee- und Lawinenforschung, No. 47. 37pp. (german)
- Sampl, P. und T. Zwinger (2004) Avalanche Simulation with SAMOS. Annals of Glaciology, 38, 393-398.
- Schaffhauser, A., Fromm, R., Jörg, P., Luzi, G., Noferini, L. and R. Sailer (submitted) Remote sensing based retrieval of snow cover properties. Submitted to Cold Regions Science and Technology.
- TIRIS (2007). [http://tiriris.tirol.gv.at/web/kartengal/karten/maxbev\\_04\\_dsr\\_a4.pdf](http://tiriris.tirol.gv.at/web/kartengal/karten/maxbev_04_dsr_a4.pdf)
- Volk, G., 2004. ELBA+ - eine neue Generation von Simulationsmodellen. Wildbach- und Lawinenverbau. 2004, 149, 55-62.
- Volk, G. and K. Kleemayr, 1999. ELBA - Ein GIS-gekoppeltes Lawinensimulationsmodell. Anwendungen und Perspektiven, in Österreichische Zeitschrift für Vermessung und Geoinformation Heft 2 + 3: 84-92.
- Zwinger, T., Kluwick, A., and P. Sampl (2003) Simulation of Dry-Snow Avalanche Flow over Natural Terrain. In Dynamic Response of Granular and Porous Materials under Large and Catastrophic Deformations, ed. K Hutter, N Kirchner. Springer, Heidelberg. 161-194.